

PV based High Step-up Input-Parallel Output-Series DC/DC Converter with Dual Coupled Inductors

M.Narsimhachary

M-tech Student Scholar

Department of Electrical & Electronics Engineering,
 Anurag College of Engineering, Aushapur, Ghatkesar;
 Rangareddy (Dt); T.S, India.
 Email:mamidojuchary@gmail.com

P.Rambabu

Assistant Professor

Department of Electrical & Electronics Engineering,
 Anurag College of Engineering, Aushapur, Ghatkesar;
 Rangareddy(Dt); T.S, India.
 Email:Ramu.rh@gmail.com

Abstract- This paper, along with the voltage multiplier chain with dual coil output to the boost converter provides a novel parallel input. On the one hand, and to take part in the input current and to reduce input current ripple in the two coils in parallel with the primary windings connected. On the other hand, it is proposed to change, and a series of interleaved output capacitors profit profitable high voltage, low output voltage ripple, low pressure switch is connected with trying gets. A coupled-inductor double-boost inverter (CIDBI) is proposed for micro inverter photovoltaic (PV) module system, and the control strategy applied to it is analyzed. Also, the operation principle of the proposed inverter is discussed and the gain from dc to ac is deduced in detail. The main attribute of the CIDBI topology is the fact that it generates an ac output voltage larger than the dc input one, depending on the instantaneous duty cycle and turns ratio of the coupled inductor as well. This paper points out that the gain is proportional to the duty cycle approximately when the duty cycle is around 0.5 and the synchronized pulse width modulation can be applicable to this novel inverter.

Key words- pv system, dc-dc converter, dual coupled output

1. INTRODUCTION

The massy usage of the fossil fuels, such as the oil, the coal and the gas, result in serious greenhouse effect and pollute the atmosphere, which has great effect on the world. Meanwhile, there is a big contradiction between the fossil Fuels supply and the global energy demand, which leads to a high oil price in the international market recently. The energy shortage and the atmosphere pollution have been the major limitations for the human development. How to find renewable energy is becoming more and more exigent [1-2].

As the output voltage of the solar panel is very low and there should be a clear transformation for such low voltage to high voltage. Hence such work could be done by boost converter. The dc-dc boost converter are used to convert the unregulated dc input to a controlled dc output at a desired voltage level. They generally perform by applying a dc voltage across an inductor or transformer a period of time (usually in the 20 kHz to 5 MHz range) which causes current to flow through it and store energy magnetically, then switching this voltage off and causing the stored energy to be transferred to the Voltage output in a

controlled manner. The output voltage is regulated by adjusting the ratio of on/off time [3-6].

Many single switch topologies based on conventional boostconverter had been presented for high step-up voltage gain. The cascaded boost converter is also capable of providing high voltage gain without the penalty of extreme duty-cycle. However, the voltage stress of the mainswitch is equal to the output voltage [7]. In references and, several switching-capacitor/switching inductor structures are proposed, and transformerless hybrid dc-dc converters with high voltage gain are derived by the use of structures integrated with classical single switch non-isolated PWM converters. They present the following advantage: the energy in the magnetic elements is low, which leads to weight, size and cost saving for the inductor, and less conduction losses [8].

Another method for achieving high step-up gain is the use of the voltage-lift technique, showing the advantage that the voltage stress across the switch is low. However, several diode-capacitor stages are required when the conversion ratio is very large, which makes the circuit complex. In addition, the single switch may suffer high current for high power applications, which risks reducing its efficiency. Another alternative single switch converters including forward, fly-back and tapped-inductor boost can achieve high conversion ratio by adjusting the turns ratio of the transformer, but these converters require large transformer turns ratio to achieve high voltage gain. In, an integrated boost-flyback converter is proposed to achieve high voltage gain, and the energy of a leakage inductor is recycled into the output during the switch-off period. Unfortunately, the input current is pulsed from the experimental results. In addition, it should be noticed that the low-level input voltages usually cause large input currents and current ripples to flow through the single switch for high step up and high power dc-dc conversion, which also leads to increasing conduction losses [9-10].



Fig.1. Block diagram

(A) DC-DC CONVERTER

Nowadays high voltage gain DC-DC converters are required in many industrial applications. Photovoltaic energy conversion systems and fuel-cell systems usually need high step up and large input current dc-dc converters to boost low voltage (18-56 V) to high voltage (200-400 V) for the grid-connected inverters. High-intensity discharge lamp ballasts for automobile headlamps call for high voltage gain DC-DC converters to raise a battery voltage of 12 V up to 100 V at steady operation. Also, the low battery voltage of 48 V needs to be converted to 380 V in the front-end stage in some uninterruptible power supplies and telecommunication systems by high step-up converters. Theoretically, a basic boost converter can provide infinite voltage gain with extremely high duty ratio. In practice, the voltage gain is limited by the parasitic elements of the power devices, inductor and capacitor. Moreover, the extremely high duty cycle operation may induce serious reverse-recovery problem of the rectifier diode and large current ripples, which increase the conduction losses. On the other hand, the input current is usually large in high output voltage and high power conversion, but low-voltage-rated power devices with small on resistances may not be selected since the voltage stress of the main switch and diode is, respectively, equivalent to the output voltage in the conventional boost converter. Many other converter topologies have developed for high step up gain. Here a high gain input-parallel output-series DC-DC converter with dual coupled inductors is designed. This configuration inherits the merits of high voltage gain, low output voltage ripple, and low voltage stress across the power switches. Moreover, the converter is able to turn ON the active switches at zero current and alleviate the reverse recovery problem of diodes by reasonable leakage inductances of the coupled inductors [11-12].

(B) Photovoltaic system

A photovoltaic system, also solar PV power system, or PV system, is a power system designed to supply usable solar power by means of photovoltaics. It consists of an arrangement of several components, including solar panels to absorb and convert sunlight into electricity, a solar inverter to change the electric current from DC to AC, as well as mounting, cabling and other electrical accessories to set up a working system. It may also use a solar tracking system to improve the system's overall performance and include an integrated battery solution, as prices for storage devices are expected to decline. Strictly speaking, a solar array only encompasses the ensemble of solar panels, the visible part of the PV system, and does not include all the other hardware, often summarized as balance of system (BOS). Moreover, PV systems convert light directly into electricity and shouldn't be confused with other technologies, such as concentrated solar power or solar thermal, used for heating and cooling.

PV systems range from small, rooftop-mounted or building-integrated systems with capacities from a few to several tens of kilowatts, to large utility-scale power stations of hundreds of megawatts. Nowadays, most PV systems are grid-connected, while off-grid or stand-alone systems only account for a small portion of the market. Operating silently and without any moving parts or environmental emissions, PV systems have developed from being niche market applications into a mature technology used for mainstream electricity generation. A rooftop system recoups the invested energy for its manufacturing and installation within 0.7 to 2 years and produces about 95 percent of net clean renewable energy over a 30-year service lifetime.[1]

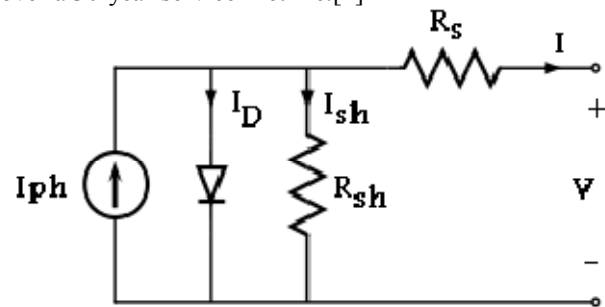


Fig 2. PV cell equivalent circuit.

Figure reflects a simple equivalent circuit of a photovoltaic cell. The current source which is driven by sunlight is connected with a real diode in parallel. In this case, PV cell presents a p-n junction characteristic of the real diode. The forward current could flow through the diode from p-side to n-side with little loss. However, if the current flows in reverse direction, only little reverse saturation current could get through.

Due to the exponential growth of photovoltaics, prices for PV systems have rapidly declined in recent years. However, they vary by market and the size of the system. In 2014, prices for residential 5-kilowatt systems in the United States were around \$3.29 per watt,[4] while in the highly penetrated German market, prices for rooftop systems of up to 100 kW declined to €1.24 per watt.[5] Nowadays, solar PV modules account for less than half of the system's overall cost,[6] leaving the rest to the remaining BOS-components and to soft costs, which include customer acquisition, permitting, inspection and interconnection, installation labor and financing costs

II. TOPOLOGY AND OPERATION PRINCIPLE OF THE PRESENTED CONVERTER

The derivation procedure for the proposed topology is shown in Fig.3. This circuit can be divided as two parts. These two segments are named a modified interleaved boost converter and a voltage doubler module using capacitor-diode and coupled inductor technologies. The basic boost converter topology shown in Fig. 3.(a) and (b) is another boost version with the same function in which

the output diode is placed on the negative dc-link rail. Fig. 3(c) is called a modified interleaved boost converter, which is an input-parallel and output-series configuration derived from two basic boost types. Therefore, this part based on interleaved control has several main functions: 1) it can obtain double voltage gain of the conventional interleaved boost; 2) low output voltage ripple due to the interleaved series connected capacitors; and 3) low switch voltage stresses. Then, the double independent inductors in the modified interleaved boost converter are separately replaced by the primary windings of coupled inductors that are employed as energy storage and filtering as shown in Fig.3 (d). The secondary windings of two coupled inductors are connected in series for a voltage multiplier module, which is stacked on the output of the modified converter to get higher voltage gain. Fortunately, this connection is also helpful to balance the currents of two primary sides. The coupling references of the inductors are denoted by the marks“*” and “.”. The equivalent circuit of the presented converter is demonstrated. Where:

- 1) L_{m1} , L_{m2} : magnetizing inductances;
- 2) L_{k1} , L_{k2} : leakage inductances;
- 3) C_1 , C_2 , C_3 : output and clamp capacitors;
- 4) S_1 , S_2 : main switches;
- 5) D_1 , D_2 : clamp diodes;
- 6) D_r , C_r : regenerative diode and capacitor;
- 7) D_3 : output diode;
- 8) N : turns ratio of N_s/N_p ;
- 9) V_{N1} , V_{N2} : the voltage on the primary sides of coupled inductors

Fig. 3.shows the theoretical waveforms when the converter is operated in continuous conduction mode (CCM). The duty cycles of the power switches are interleaved with 180° phase shift, and the duty cycles are greater than 0.5. That is to say, the two switches can only be in one of three states (S_1 : ON, S_2 : ON; S_1 : ON, S_2 : OFF; S_1 : OFF, S_2 : ON), which ensures the normal transmission of energy from the coupled inductor's primary side to the secondary one. The operating stages can be found in Figs.4.

- 1) **First stage [t_0-t_1]:** At $t = t_0$, the power switch S_1 is turned on with zero-current switching (ZCS) due to the leakage inductance L_{k1} , while S_2 remains turned ON, as shown in Fig. 4. Diodes D_1, D_2 , and D_r are turned OFF, and only output diode D_3 is conducting. The current falling rate through the output diode D_3 is controlled by the leakage inductances L_{k1} and L_{k2} , which alleviates the diodes' reverse recovery problem. This stage ends when the current through the diode D_3 decreases to zero.
- 2) **Second stage [t_1-t_2]:** During this interval, both the power switches S_1 and S_2 are maintained turned ON, as shown in Fig.5 All of the diodes are reversed-biased. The magnetizing inductances L_{m1} and L_{m2} as well as leakage inductances L_{k1} and L_{k2} are linearly charged

by the input voltage source V_{in} . This period ends at the instant t_2 , when the switch S_2 is turned OFF.

- 3) **Third stage [t_2-t_3]:** At $t = t_2$, the switch S_2 is turned OFF, which makes the diodes D_2 and D_r turned ON. The current flow path is shown in Fig.6. The energy that magnetizing inductance L_{m2} has stored is transferred to the secondary side charging the capacitor C_r by the diode D_r , and the current through the diode D_r and the capacitor C_r is determined by the leakage inductances L_{k1} and L_{k2} . The input voltage source, magnetizing inductance L_{m2} and leakage inductance L_{k2} release energy to the capacitor C_2 via diode D_2 .
- 4) **Fourth stage [t_3-t_4]:** At $t = t_3$, diode D_2 automatically switches OFF because the total energy of leakage inductance L_{k2} has been completely released to the capacitor C_2 . There is no reverse recovery problem for the diode D_2 . The current-flow path of this stage is shown in Fig.7. Magnetizing inductance L_{m2} still transfers energy to the secondary side charging the capacitor C_r via diode D_r . The current of the switch S_1 is equal to the summation of the currents of the magnetizing inductances L_{m1} and L_{m2} .
- 5)

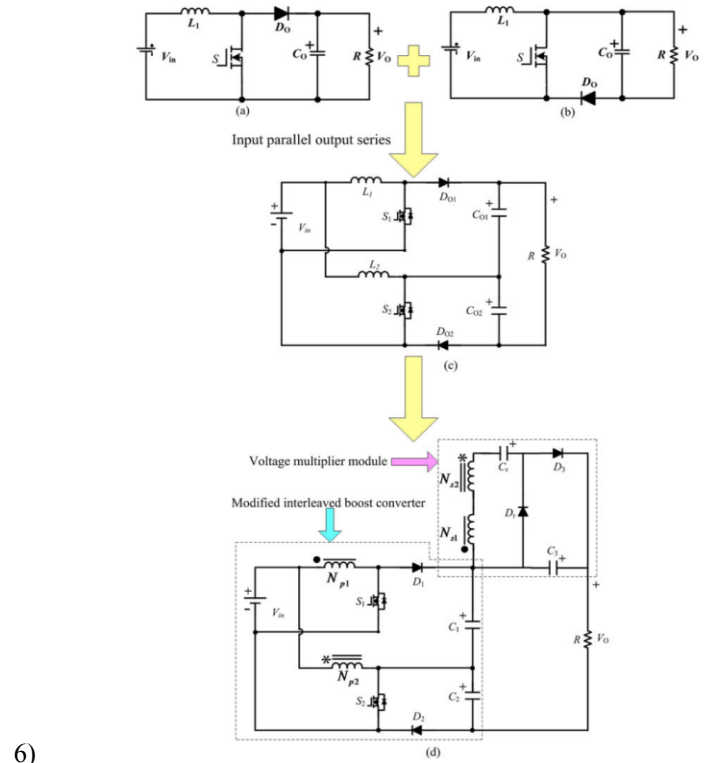


Fig. 3. Procedure to obtain the proposed converter with high voltage gain. (a) Conventional boost converter. (b) Other structure of boost converter. (c) Modified interleaved boost. (d) High gain input-parallel output-series dc/dc converter with dual coupled inductors.

- 7) **Fifth stage [t_4-t_5]:** At $t = t_4$, the switch S_2 is turned ON with ZCS soft-switching condition. Due to the leakage inductance L_{k2} and the switch S_1 remains in ON

state. The current flow path of this stage is shown in Fig. 8. The current falling rate through the diode D_r is controlled by the leakage inductances L_{k1} and L_{k2} , which alleviates the diode reverse recovery problem. This stage ends when the current through the diode D_r decreases to zero at $t = t_5$.

8) **Sixth stage [t5–t6]:** The operating states of stages 6 and 2 are similar. During this interval, all diodes are turned OFF. The magnetizing inductances L_{m1} and L_{m2} , and the leakage inductances L_{k1} and L_{k2} are charged linearly by the input voltage. The voltage stress of $D1$ is the voltage on $C1$, and the voltage stress of $D2$ is the voltage on $C2$. The voltage stress of D_r is equivalent to the voltage on C_r , and the voltage stress of $D3$ is the output voltage minus the voltages on $C1$ and $C2$ and C_r .

9) **Seventh stage [t6–t7]:** The power switch $S1$ is turned OFF at $t = t_6$, which turns ON $D1$ and $D3$, and the switch $S2$ remains in conducting state. The current-flow path of this stage is shown in Fig. 10. The input voltage source V_{in} , magnetizing inductance L_{m1} and leakage inductance L_{k1} release their energy to the capacitor $C1$ via the switch $S2$. Simultaneously, the energy stored in magnetizing inductor L_{m1} is transferred to the secondary side. The current through the secondary sides in series flows to the capacitor $C3$ and load through the diode $D3$.

10) **Eighth stage [t7–t0]:** At $t = t_7$, since the total energy of leakage inductance L_{k1} has been completely released to the capacitor $C1$, diode $D1$ automatically switches OFF. The current of the magnetizing inductance L_{m1} is directly transferred to the output through the secondary side of coupled inductor and $D4$ until t_0 .

It should be pointed out that the time periods of stages I, IV, V, and VIII are much shorter than those shown in Fig. 3., which were enlarged in order to clearly show the waveform variations.

III. STEADY-STATE PERFORMANCE ANALYSIS OF THE PROPOSED CONVERTER

To simplify the circuit performance analysis of the proposed converter in CCM, the following conditions are assumed.

- 1) All of the power devices are ideal. That is to say, the on-state resistance R_{DS} (ON) and all parasitic capacitors of the main switches are neglected, and the forward voltage drop of the diodes is ignored.
- 2) The coupling-coefficient k of each coupled inductor is defined as $L_m/(L_m + L_k)$. The turn ratio N of each coupled inductor is equal to N_S/N_P .
- 3) The parameters of two coupled inductors are considered to be the same, namely $L_{m1} = L_{m2} = L_m$, $L_{k1} = L_{k2} = L_k$, $N_{S1}/N_{P1} = N_{S2}/N_{P2} = N$, and $k_1 = L_{m1}/(L_{m1} + L_{k1}) = k_2 = L_{m2}/(L_{m2} + L_{k2}) = k$.
- 4) Capacitors $C1$, $C2$, $C3$, and C_r are large enough. Thus, the voltages across these capacitors are considered as constant in one switching period.

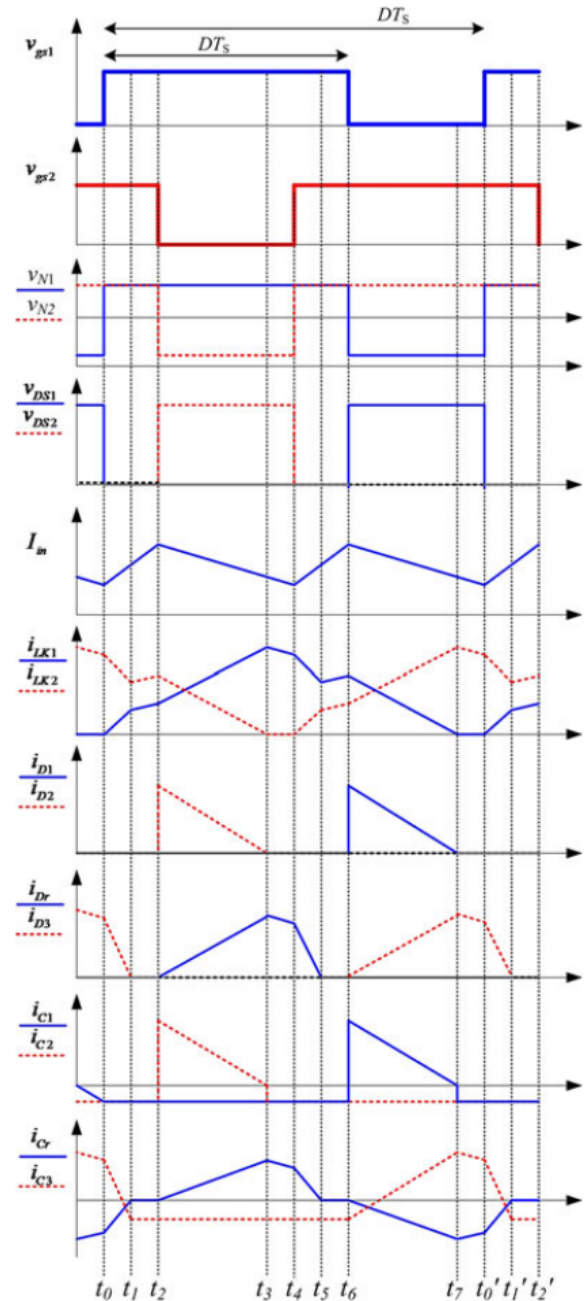


Fig. 4. Key theoretical waveforms.

(A) Voltage Gain Expression

If the transient characteristics of circuit are disregarded, each magnetizing inductance has two main states in one switching period. In one state, the magnetizing inductance is charged by the input source. In the other state, the magnetizing inductance is discharged by the output capacitor voltage V_{C1} or V_{C2} minus the input voltage. Since the time durations of stages I, IV, V, and VIII are significantly short, only stages II, III, VI, and VII

areconsidered for the steady-state analysis. At stages II and VI, the

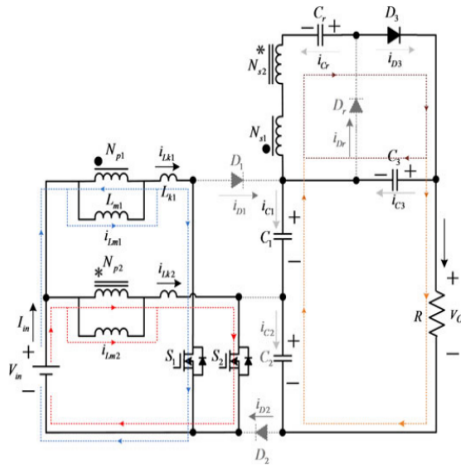


Fig.5. First stage

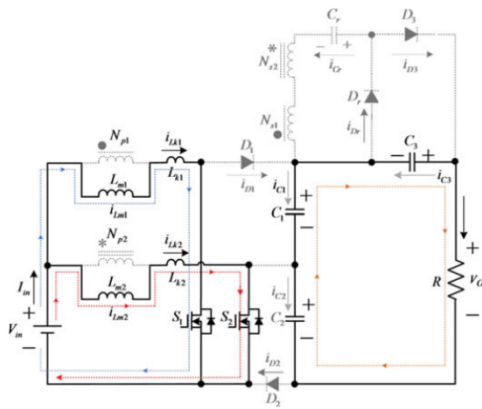


Fig.6. Second stage

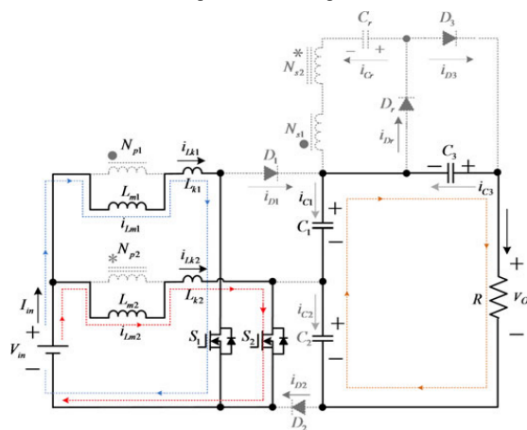


Fig.7. Second stage

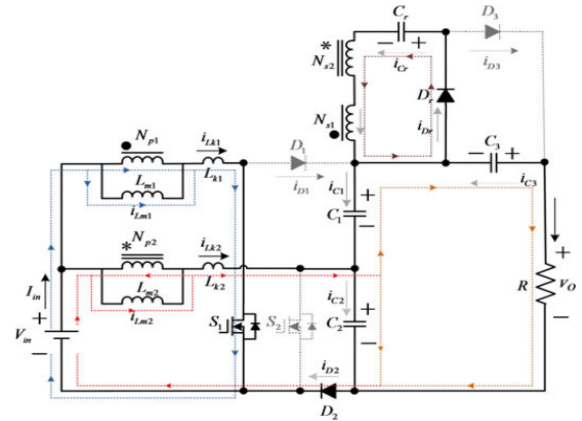


Fig.8. Third stage.

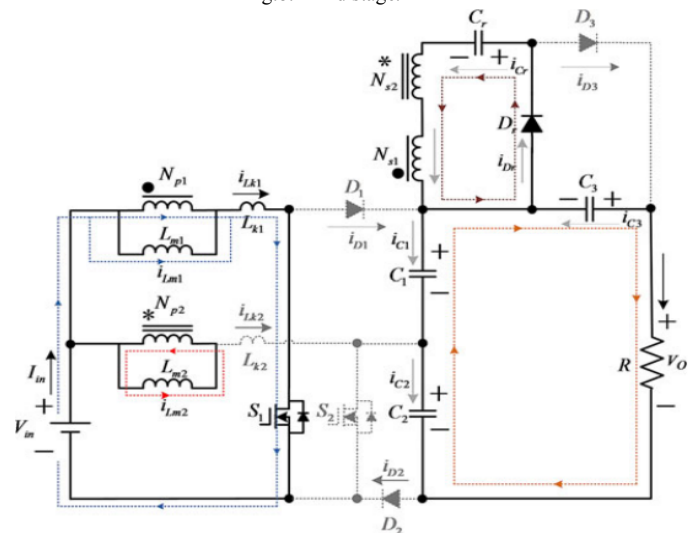


Fig.9. Fourth stage

Following equations can be written from Figs.5 and 9

$$V_{Lm1}^{II} = V_{Lm1}^{VI} = kV_{in} \quad (1)$$

$$V_{Lm2}^{II} = V_{Lm2}^{VI} = kV_{in} \quad (2)$$

$$V_o = V_{C1} + V_{C2} + V_{C3} \quad (3)$$

At stage III, the following equations are derived from Fig.6:

$$V_{Lm1}^{III} = kV_{in} \quad (4)$$

$$V_{Lm2}^{III} = k(V_{in} - V_{C2}) \quad (5)$$

$$V_{Cr} = V_{S1} - V_{S2} = kNV_{C2} \quad (6)$$

During the time duration of stage VII, the following voltage equations can be expressed based on Fig. 10:

$$V_{Lm1}^{VII} = k(V_{in} - V_{C1}) \quad (7)$$

$$V_{Lm2}^{VII} = kV_{in} \quad (8)$$

$$V_{C3} = V_{Cr} + V_{S2} - V_{S1} = kN(V_{C1} + V_{C2}) \quad (9)$$

Using the volt-second balance principle on Lm1 and Lm2, respectively, the following equation is derived:

$$\int_0^{\frac{(2D-1)T}{2}} V_{Lm1}^{II} dt + \int_0^{(1-D)T} V_{Lm1}^{III} dt + \int_0^{\frac{(2D-1)T}{2}} V_{Lm1}^{VI} dt + \int_0^{(1-D)T} V_{Lm1}^{VII} dt = 0 \quad (10)$$

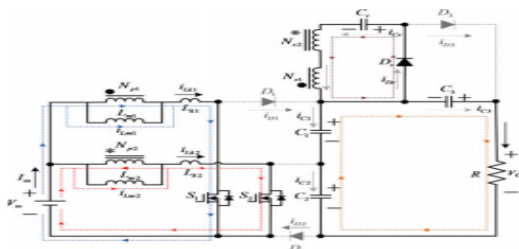


Fig.10. Fifth stage.

IV. MATLAB/SIMULATION RESULTS

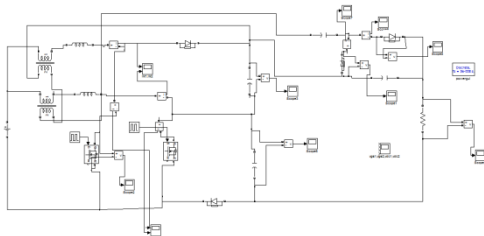


Fig 11 Matlab/simulation circuit of High Step-up Input-Parallel Output-Series DC/DC Converter with Dual Coupled Inductors.

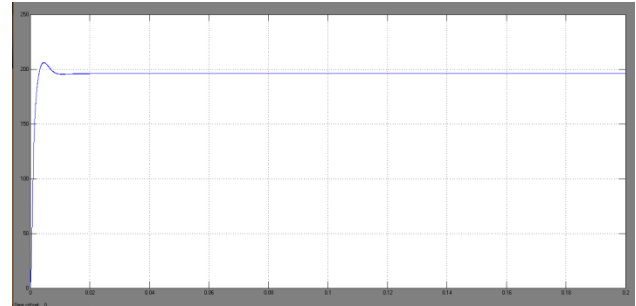


Fig 12 simulation wave form output voltage

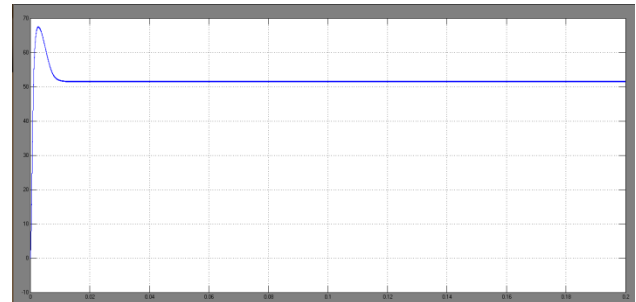


Fig 13 simulation wave form couple of inductance voltage

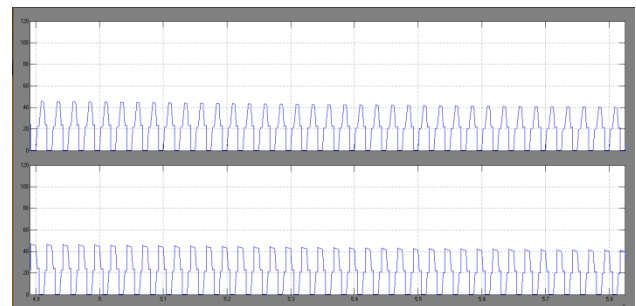


Fig 14 simulation wave form couple of inductance current

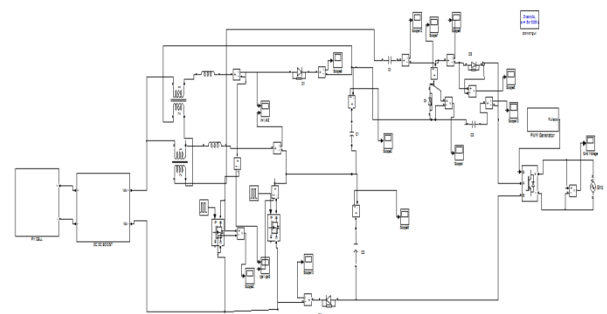


Fig 15 Matlab/simulation circuit of High Step-up Input-Parallel Output-Series DC/DC Converter with Dual Coupled Inductors with PV



Fig 16 simulation wave form of High Step-up Input-Parallel Output-Series DC/DC Converter with Dual Coupled Inductors with PV output voltage

V. CONCLUSION

Low input voltage and high energy step changes, this paper successfully developed and series' inductor production volumes and parallel input techniques as high-voltage Converter has been achieved. The proposed dc converter is simple in construction and has more efficiency than the conventional dc-dc converter. This can be used in battery operated vehicles, and solar powered uninterrupted power supplies and can have significant use in renewable energy sources where there is a need of efficient dc conversion. The key theoretical waveforms, steady-state operational principle, and the main circuit performance are discussed to explore the advantages of the proposed converter. Performance of the converter is simulated using MATLAB/SIMULINK software.

REFERENCES

- [1] C. Cecati, F. Ciancetta, and P. Siano, "A multilevel inverter for photovoltaic systems with fuzzy logic control," *IEEE Trans. Ind. Electron.*, vol. 57, no. 12, pp. 4115–4125, Dec. 2010.
- [2] X. H. Yu, C. Cecati, T. Dillon, and M. G. Simoes, "The new frontier of smart grid," *IEEE Trans. Ind. Electron. Mag.*, vol. 15, no. 3, pp. 49–63, Sep. 2011.
- [3] G. Fontes, C. Turpin, S. Astier, and T. A. Meynard, "Interactions between fuel cell and power converters: Influence of current harmonics on a fuel cell stack," *IEEE Trans. Power Electron.*, vol. 22, no. 2, pp. 670–678, Mar. 2007.
- [4] J. Y. Lee and S. N. Hwang, "Non-isolated high-gain boost converter using voltage-stacking cell," *Electron. Lett.*, vol. 44, no. 10, pp. 644–645, May 2008.
- [5] Z. Amjadi and S. S. Williamson, "Power-electronics-based solutions for plug-in hybrid electric vehicle energy storage and management systems," *IEEE Trans. Ind. Electron.*, vol. 57, no. 2, pp. 608–616, Feb. 2010.
- [6] L. Henrique, S. C. Barreto, P. P. Praca, D. S. Oliveira Jr., and R. N. A. L. Silva, "High-voltage gain boost converter based on three-state commutation cell for battery charging using PV panels in a single conversion stage," *IEEE Trans. Power Electron.*, vol. 29, no. 1, pp. 150–158, Jan. 2014.
- [7] F. Boico, B. Lehman, and K. Shujaee, "Solar battery chargers for NiMH batteries," *IEEE Trans. Power Electron.*, vol. 22, no. 5, pp. 1600–1609, Sep. 2007.
- [8] A. Reatti, "Low-cost high power-density electronic ballast for automotive HID lamp," *IEEE Trans. Power Electron.*, vol. 15, no. 2, pp. 361–368, Mar. 2000.

[9] A. I. Bratcu, I. Munteanu, S. Bacha, D. Picault, and B. Raison, "Cascaded DC-DC converter photovoltaic systems: Power optimization issues," *IEEE Trans. Ind. Electron.*, vol. 58, no. 2, pp. 403–411, Feb. 2011.

[10] H. Tao, J. L. Duarte, and M. A. M. Hendrix, "Line-interactive UPS using a fuel cell as the primary source," *IEEE Trans. Ind. Electron.*, vol. 55, no. 8, pp. 3012–3021, Aug. 2008.

[11] Y. P. Hsieh, J. F. Chen, T. J. Liang, and L. S. Yang, "Novel high step-up DC-DC converter for distributed generation system," *IEEE Trans. Ind. Electron.*, vol. 60, no. 4, pp. 1473–1482, Apr. 2013.

[12] M. H. Todorovic, L. Palma, and P. N. Enjeti, "Design of a wide input range dc-dc converter with a robust power control scheme suitable for fuel cell power conversion," *IEEE Trans. Ind. Electron.*, vol. 55, no. 3, pp. 1247–1255, Mar. 2008.

Author's Profile:



M.narsimhachary received B-tech from Gandhi Academy of technical Education in the year 2008 and now pursuing M.Tech in the stream of Power electronic and electrical drives at Anurag College of Engineering.



P.Rambabure received M.TECH degree from Vardhaman College of Engineering in the year 2010 and M.Tech in the stream of Power electronic and electrical drives. Currently working as a Assistant Professor in Anurag College of Engineering since 3 years and I am also the member of ISTE.

And his areas of interest are Power electronics, Electrical machines, Electrical Circuits and Control Systems.